Spectrochimica Acta Part A 81 (2011) 59–63

Contents lists available at ScienceDirect

Spectrochimica Acta Part A: Molecular and Biomolecular Spectroscopy

journal homepage: www.elsevier.com/locate/saa

EPR, thermo and photoluminescence properties of ZnO nanopowders

A. Jagannatha Reddy[a], M.K. Kokila[b,*], H. Nagabhushana[c], J.L. Rao[d], C. Shivakumara[e], B.M. Nagabhushana[f], R.P.S. Chakradhar[g,**]

[a] Department of Physics, M.S. Ramaiah Institute of Technology, Bangalore 560 054, India
[b] Department of Physics, Bangalore University, Bangalore 560 056, India
[c] Prof. C.N.R. Rao Centre for Advanced Materials Research, Tumkur University, Tumkur 572103, India
[d] Department of Physics, S.V. University, Tirupathi 517 502, India
[e] Solid State and Structural Chemistry Unit, Indian Institute of Science, Bangalore 560 012, India
[f] Department of Chemistry, M.S. Ramaiah Institute of Technology, Bangalore 560 054, India
[g] National Aerospace Laboratories (CSIR), Bangalore 560017, India

ARTICLE INFO

Article history:
Received 17 May 2011
Accepted 18 May 2011

Keywords:
ZnO
Photoluminescence
Thermoluminescence
Electron paramagnetic resonance

ABSTRACT

Nanocrystalline ZnO powders have been synthesized by a low temperature solution combustion method. The photoluminescence (PL) spectrum of as-formed and heat treated ZnO shows strong violet (402, 421, 437, 485 nm) and weak green (520 nm) emission peaks respectively. The PL intensities of defect related emission bands decrease with calcinations temperature indicating the decrease of Zn_i and V_o^+ caused by the chemisorptions of oxygen. The results are correlated with the electron paramagnetic resonance (EPR) studies. Thermoluminescence (TL) glow curves of gamma irradiated ZnO nanoparticles exhibit a single broad glow peak at ~343 °C. This can be attributed to the recombination of charge carriers released from the surface states associated with oxygen defects, mainly interstitial oxygen ion centers. The trapping parameters of ZnO irradiated with various γ-doses are calculated using peak shape method. It is observed that the glow peak intensity increases with increase of gamma dose without changing glow curve shape. These two characteristic properties such as TL intensity increases with gamma dose and simple glow curve structure is an indication that the synthesized ZnO nanoparticles might be used as good TL dosimeter for high temperature application.

© 2011 Elsevier B.V. All rights reserved.

1. Introduction

ZnO is an n-type II–VI semiconductor and has rapidly emerged as a promising optoelectronic material due to its large direct band gap of 3.37 eV, low power threshold for optical pumping at room temperature, highly efficient UV emission resulting from a large exciton binding energy at room temperature. This large exciton binding energy provides excitonic emission more efficiently even at higher temperature. Thus wurtzite structured ZnO is of potential importance for its application in light emitting diodes (LEDs), laser diodes (LDs) and ultra-violet (UV) photo detectors [1–4].

The possibility of tailor making bulk material properties by varying size, structure and composition of constituting nanoscale particles makes them candidates for various important applications in the field of materials research. Zhou et al. [5] synthesized ZnO nanoparticles by gel-template combustion method and investigated the influence of heating conditions on size and photoluminescence of ZnO nanoparticles. Fan et al. [6] synthesized ZnO nanorods with hexagonal structures by the hydrothermal method at different conditions and studied their room temperature emission spectra and fluorescent dynamics. Salavati-Niasari et al. [7] prepared ZnO nanotriangles by thermal decomposition and studied their photocatalytic activity. Risti et al. [8] synthesized ZnO nanopowders by sol–gel synthesis and Raman spectra of ZnO particles were interpreted taking into account the nanosize effect. Chen et al. [9] prepared ZnO nanoparticles by direct precipitation method, Aimable et al. [10] synthesized ZnO nanoparticles by polymer-assisted precipitation in mild hydrothermal conditions and the influence of soft templates (organic species) to control size and size distribution in the final product was investigated.

In the present study, we report the photoluminescence (PL) and thermoluminescence (TL) properties of spherical shaped nanocrystalline ZnO powders prepared via low temperature solution combustion method. Thermoluminescence (TL), also known as thermally stimulated luminescence (TSL) is widely used to study defects in insulators and semiconducting materials. Moreover, this method is successfully applied in the field of radiation dosimetry. ZnO is inert to environmental conditions, nontoxic and insoluble

* Corresponding author.
** Corresponding author. Tel.: +91 080 2508 6251.
E-mail addresses: drmkkokila@gmail.com (M.K. Kokila), sreechakra72@yahoo.com (R.P.S. Chakradhar).

1386-1425/$ – see front matter © 2011 Elsevier B.V. All rights reserved.
doi:10.1016/j.saa.2011.06.048

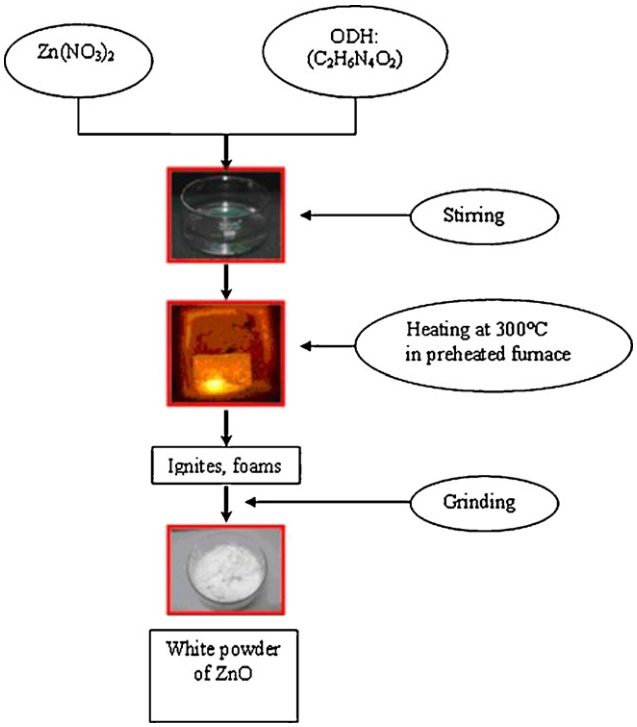

Fig. 1. Flowchart for the synthesis of combustion derived ZnO nanopowder.

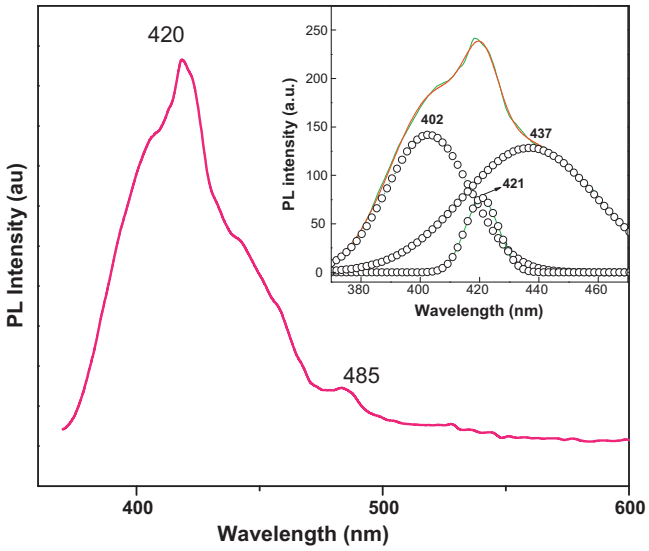

Fig. 2. PL spectrum of as-formed ZnO (inset) deconvoluted curves.

in water. In spite of these characteristics, there is not much information related to the potential application of ZnO in TL dosimetry. The lack of interest of ZnO as dosimetric material is due perhaps to its other important applications. However, all the past works have been carried out on beta and X-ray irradiation [11–13] and there are no reports on γ-ray irradiation. In this paper, we report for first time the thermo luminescent properties of ZnO nanopowders irradiated by γ-rays. We have also examined the intrinsic defects in ZnO like zinc or oxygen vacancies present in this material using Electron paramagnetic resonance (EPR) spectroscopy and the results are discussed in detail.

2. Experimental

Fig. 1 shows the flow chart for the preparation of ZnO nanopowders. All the chemical reagents used in the present experiments were of analytical grade and used without further purification. Stoichiometric amounts of $Zn(NO_3)_2{\cdot}6H_2O$ and the fuel $C_2H_6N_4O_2$ were dissolved in doubled distilled water in a cylindrical petri dish and heated in muffle furnace set at 300 °C. A detailed synthesis procedure of ZnO nanopowders and its characterization (PXRD, SEM, TEM, FTIR, UV–vis and Raman) is available in our earlier report. The photoluminescence measurements were carried out using Perkin–Elmer LS-55 spectrophotometer equipped with Xe lamp source with 254 nm excitation wavelength. TL measurements were carried out at room temperature using Nucleonix TL reader using (^{60}Co) gamma source as excitation in the dose range 10–50 Gy. The EPR spectrum was recorded at room temperature using a JEOL-FE-1X EPR spectrometer operating in the X-band frequency (≈9.200 GHz) with a field modulation frequency of 100 kHz. The magnetic field was scanned from 0 to 500 mT and the microwave power used was 5 mW. A powdered specimen of 100 mg was taken in a quartz tube for EPR measurements.

3. Results and discussion

3.1. Photoluminescence (PL) studies

Fig. 2 shows the PL spectrum of the as-formed ZnO nanopowders. Upon 254 nm excitation, the emission spectrum of ZnO has the asymmetric curve in the visible region, which implies the superposition of multiple emission bands. Gaussian curve fitting was applied to deconvolute the PL curve. The PL spectrum shows a violet emission peak at ~402 nm, blue emission peaks at ~421, 437, 485 nm and weak green emission peak at ~525 nm. The violet emission corresponds to the near band edge emission of the wide band gap of ZnO due to the annihilation of exciton. The broad blue band emissions are possibly due to surface defects in the ZnO such as oxygen vacancies (V_o) and Zinc interstitials (Zn_i). The green luminescence is associated with the intrinsic defect centers such as oxygen vacancies, zinc vacancies, zinc interstitials or oxygen interstitials [14,15]. Though the origin of green emission is generally attributed to deep level or trapped state emission, there is no universally accepted mechanism. The commonly cited explanation is that green emission originates from the radiative recombination of a photo-generated hole with an electron occupying the oxygen vacancy. Niu et al. [16] and Ghoshal et al. [17] reported that the green luminescence might be due to the transition from the conduction band to the deeply trapped hole. Complex defects involving the transition from the zinc interstitials to the deep acceptor levels such as oxygen vacancies constitute another explanation for the green emission. Our EPR study gives further evidence of surface defects in ZnO nanopowders, which will be dealt with in subsequent sections.

The room temperature PL spectra of ZnO nanopowders prepared at different annealing temperatures (500, 700 and 1000 °C) are shown in Fig. 3. The PL spectra showed the near band edge UV emission and defect related blue and green emissions compared to the as-formed sample. A red shift of the near band edge emission bands were observed in the post annealed ZnO nanoparticles. The former phenomena can be attributed to quantum confinement effect with an increase in crystal dimension and the later can be attributed to the decrease of Zn_i and V_o^+ caused by the chemisorptions of oxygen.

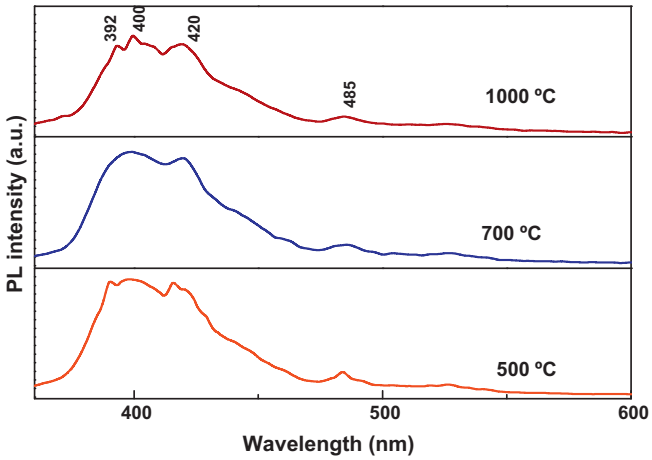

Fig. 3. PL spectra of ZnO annealed at different temperatures.

3.2. Thermoluminescence (TL) studies

Fig. 4 shows the thermoluminescence (TL) spectra of ZnO nanopowders irradiated with gamma (γ) rays for a dose range of 10–50 Gy. A well resolved broad single glow peak at ~343 °C was observed for all the samples. This is attributed to the recombination of charge carriers released form the surface states associated with oxygen defects, mainly interstitial oxygen ion centers. It is observed that the glow peak intensity increases with increase of gamma dose without changing glow curve shape. The increase in intensity of TL glow peak with irradiation dose can be understood by the fact that more and more traps responsible for the glow peak are getting filled with the increase of irradiation dose and subsequently these traps release the charge carriers on thermal stimulation to finally recombine with their counterparts, thus giving rise to glow peaks. These two properties (i) TL intensity increases with gamma dose and (ii) simple glow curve structure is an indication that the combustion synthesized ZnO nanopowders might be used as good TL dosimeter for high temperature.

TL dosimetry has become a reliable and routine method for measuring ionizing radiations. Significant advancements have been made in TL experiments during last few years. There are many commercially available TL dosimeters by different trade names. It

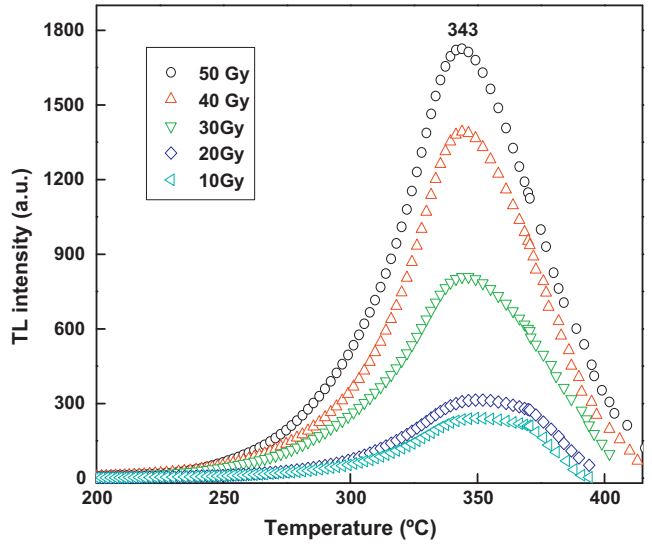

Fig. 4. TL glow curves of ZnO nanocrystals irradiated with γ-rays.

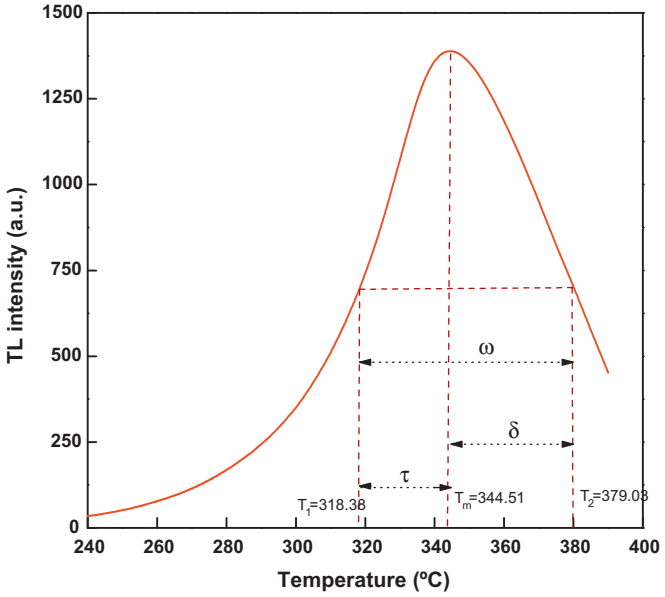

Fig. 5. TL glow peak for calculation of trapping parameters.

has been established that the optical properties of materials in the nanoscale region can be very different from those of bulk equivalent. These studies state that the nanomaterials have potential application in dosimetry of ionizing radiation where the commercial microcrystalline phosphors do not meet the requirements. Decreasing the particle size causes increasing of both the number of surface states and the proportion of recombination of charge carriers.

Cruz-Vazquez et al. [12] studied TL properties of ZnO nanophosphors irradiated with beta rays in the dose range 0.15–10.5 kGy. A well intense TL glow peak is recorded at ~220 °C. The glow curves exhibits a complex structure in the form of broad curve indicating the overlapping of several TL glow peaks. Further, ZnO nanopowder exhibited super linear dependence as a function of irradiation dose. Same authors have studied [11] thermo stimulated luminescence (TSL) of microcrystalline ZnO–$CdSO_4$ composites exposed to beta irradiation (50–300 Gy). The glow curve exhibited two maxima centered around 112 and 216 °C. The glow peak shape is quite different to that of ZnO. Zinc oxide exhibited a very complex glow curve composed of several overlapped peaks, which makes very difficult to analyze the dosimetric parameters. They recorded glow peaks at 112, 140, 216 °C. Secu and Mariana Sima [18] recorded PL and TL of ZnO nano needle arrays and films. ZnO polycrystalline powder shows a strong TL peak at ~380 °C with shoulder peak at lower temperature. The TL peak is rather similar to that, one recorded on ZnO nano needles, except for a small shift towards higher temperatures. This might suggest a linkage of the defects and TL mechanism. Indeed oxygen vacancies or vacancy interstitial pairs have been observed.

A detailed TL characteristic of the ZnO nanopowder requires the knowledge of trapping parameters. Such as activation energy (E), of the traps involved in TL emission, and order of kinetics (b) associated with the glow peaks. Here, E is a measure of the energy required to eject an electron from the defect center to the conduction band and s is the rate of electron ejection. The order of kinetics b is a measure of the probability that a free electron gets retrapped. This retrapping effect increases with density of empty traps. The trapping parameters were calculated using Chen's set of empirical formulae [19] for the peak shape method as summarized below. Fig. 5 shows the schematic representation of TL glow peak for calculation of trapping parameters.

Table 1
Trap parameters of as-formed ZnO at an heating rate (β) of 6.7 °C s^{-1}.

Gamma dosage (Gy)	T_m (°C)	Form factor, μ_g	Order of kinetics, b	Activation energy (eV)				Frequency factor, s (s^{-1})
				E_τ	E_δ	E_ω	E_{Avg}	
10	350	0.49	2	0.4912	0.5402	0.5173	0.5162	8.25×10^6
20	351	0.51	2	0.4748	0.5203	0.4997	0.4983	4.141×10^6
30	345	0.54	2	0.5144	0.5266	0.5213	0.5208	12.835×10^6
40	345	0.56	2	0.6311	0.5843	0.5925	0.6026	2.375×10^8
50	344	0.53	2	0.5248	0.5325	0.5292	0.5288	18.13×10^6

The activation energy (E)

$$E_\alpha = c_\alpha \left(\frac{kT_m^2}{\alpha} \right) - b_\alpha (2kT_m) \quad (1)$$

where $\alpha = \tau, \delta, \omega$ with $\tau = T_m - T_1$, $\delta = T_2 - T_m$, $\omega = T_2 - T_1$

$$\begin{aligned} C_\tau &= 1.51 + 3.0(\mu_g - 0.42), & b_\tau &= 1.58 + 4.2(\mu_g - 0.42) \\ C_\delta &= 0.976 + 7.3(\mu_g - 0.42), & b_\delta &= 0 \\ C_\omega &= 2.52 + 10.2(\mu_g - 0.42), & b_\omega &= 1 \end{aligned} \quad (2)$$

The form factor (symmetry factor) (b)

$$\mu_g = \frac{T_2 - T_m}{T_2 - T_1} \quad (3)$$

The nature of the kinetics can be found by the form factor. Theoretically the value of geometrical form factor (μ_g) is close to 0.42 for first order kinetics and 0.52 for second order kinetics. In the present study, the value of μ_g is very close to 0.52 and it falls under second order kinetics. The average activation energy (E) of ZnO was found to be ~0.5162–0.5288 eV. The trapping parameters of ZnO irradiated with various γ-doses obtained using peak shape method is given in Table 1.

3.3. Electron paramagnetic resonance (EPR) studies

EPR provides a sensitive and direct method to monitor various behaviors to the presence of native defects, such as oxygen vacancies and zinc vacancies. In fact, most of the experimental investigations of oxygen vacancies in ZnO to date have relied on the EPR measurements. In the bulk ZnO single crystals, the EPR resonance of shallow donors is typically detected at $g = 1.956$ and it shows a slight anisotropy due to the wurzite crystal structure. In most of the investigations of ZnO samples, the EPR line near $g = 1.96$ which is common in ceramics and powders. This line consists of several components with g factors close to $g_\parallel = 1.957$ and $g_\perp = 1.955$ of shallow donors in single ZnO crystals [20]. The nature of these components is not well established. Probably they are related to different shallow donors localized in the bulk of the ZnO and on or near the surface of ZnO particles. In many reports, the $g = 1.96$ line is attributed to positively charged oxygen vacancy but detail analysis [21–23] shows that it can be related rather to conduction electrons located at donor centers in bulk and surface center of ZnO particles. An EPR signal with $g_\parallel = 1.994$ and $g_\perp = 1.996$ has been unambiguously assigned to singly ionized oxygen vacancies [24–26]. An EPR spectrum with g values ranging from 2.003 to 2.019 has been assigned to the singly ionized zinc vacancy in ZnO [27–29]

Fig. 6 shows the EPR spectrum of as-formed ZnO nanocrystalline powder recorded at room temperature. The EPR spectrum exhibits intense sharp resonance signals at $g = 1.994$ and $g \sim 2.007$. In addition, broad resonance signals at $g = 2.540$, $g = 2.145$ and $g = 1.775$ have also been observed. The narrow resonance signal at $g \sim 1.994$ has been assigned to V_o^+ singly ionized oxygen in ZnO. The other resonance signals at $g \sim 2.007$ and $g = 2.145$ have been attributed to Zn vacancy. The origin of other signals at $g = 2.540$ and $g = 1.775$ is not known. For nanocrystal diameters which are closure to the Bohr radius in ZnO (i.e., 1.5 nm) one can expect quantum size effects. This

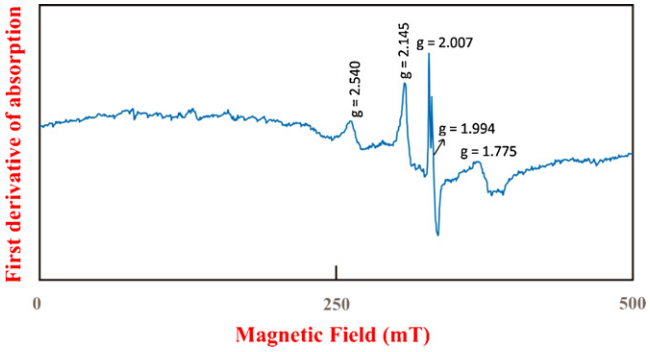

Fig. 6. EPR spectrum of as-formed ZnO nanopowder at room temperature.

shows up in the EPR experiments by the fact that the resonance is shifted towards $g \sim 2.00$. The deviation of g-value from the free electron value ($g = 2.0023$, pure s-type wave function) is caused by the admixture of valence band and higher lying conduction band states.

4. Conclusions

Hexagonal wurtzite structure ZnO nanopowders were prepared by combustion technique. The PL spectrum of ZnO nanopowders gives the near band edge UV emission and defect related blue and green emissions. EPR studies also confirm the formation of defects in ZnO nanopowders. TL glow curves of gamma irradiated ZnO nanoparticles shows a broad peak at ~343 °C, which is attributed to the recombination of charge carriers released from the surface states associated with oxygen defects, mainly interstitial oxygen ion centers for a dose range of 10–50 Gy. It is observed that the glow peak intensity increases with increase of gamma dose without changing glow curve shape. These two characteristic properties such as TL intensity increases with gamma dose and simple glow curve structure is an indication that the combustion synthesized ZnO nanopowders might be used as good TL dosimeter for high temperature application. Further, the detailed dosimetric characteristic properties with wide range of irradiation are in progress.

Acknowledgements

Dr. B.M. Nagabhushana gratefully acknowledges Visvesvaraya Technological University, Belgaum, for the financial support (VTU/2009-10/A-9/11714) to carryout this research work. Dr. H. Nagabhushana thanks Dr. S.C. Sharma, Vice-chancellor, Tumkur University, Tumkur, for constant encouragement and support. A. Jagannatha Reddy express his gratitude to Dr. M. Suguna, for fruitful discussions regarding nanomaterials.

References

[1] G.R. Gattorno, P.S. Jacinto, L.R. Va'zquez, J. Phys. Chem. B 107 (2003) 12597.
[2] E. Meulenkamp, J. Phys. Chem. B 102 (1998) 5566.

[3] M.H. Huang, S. Mao, H. Feick, H. Yan, Y. Wu, H. Kind, E. Weber, R. Russo, P. Yang, Science 292 (2001) 1897.
[4] C.R. Gorla, N.W. Emanetoglu, S. Liang, W.E. Mayo, Y. Lu, M. Wraback, H. Shen, J. Appl. Phys. 85 (1999) 2595.
[5] J. Zhou, Y. Wang, F. Zhao, Y. Wang, Y. Zhang, L. Yang, J. Lumin. 119–120 (2006) 248.
[6] L. Fan, H. Song, T. Li, L. Yu, Z. Liu, G. Pan, Y. Lei, X. Bai, T. Wang, Z. Zheng, X. Kong, J. Lumin. 122 (2007) 819.
[7] S.-N. Masoud, N. Mir, F. Davar, J Alloys Compd. 476 (2009) 908.
[8] M. Ristiĭ, S. Musi, M. Ivanda, S. Popovi, J. Alloys Compd. 397 (2005) L1.
[9] C.C. Chen, P. Liu, C.H. Lu, J. Chem. Eng. 144 (2008) 509.
[10] A. Aimable, M.T. Buscaglia, V. Buscaglia, P. Bowen, J. Eur. Ceram. Soc. 30 (2010) 591.
[11] C. Cruz-Vázquez, V.R. Orante-Barrón, H. Grijalva-Monteverde, V.M. Castaño, R. Bernal, Mater. Lett. 61 (2007) 1097.
[12] C. Cruz-Vaĭzquez, R. Bernal, S.E. Burruel-Ibarra, H. Grijalva-Monteverde, M. Barboza-Flores, Opt. Mater. 27 (2005) 1235.
[13] A.K. Srivastava, K. Ninagawa, S. Toyoda, B.R. Chakraborty, S. Chandra, Opt. Mater. 32 (2009) 410.
[14] V.S. Gorelik, S.N. Mikov, M.I. Sokolovskii, T. Tsuzuki, Inorg. Mater. 42 (2006) 282–285.
[15] S.A. Shojaee, M.M. Shahraki, M.A. Faghihi Sani, A. Nemati, A. Yousefi, J. Mater. Sci. Mater. Electron. 21 (2010) 571–577.
[16] H. Niu, Q. Yang, F. Yu, K. Tang, Yi. Xie, Mater. Lett. 61 (2007) 137–140.
[17] T. Ghoshal, S. Kar, S. Chaudhuri, Cryst. Growth Des. 7 (2007) 136–141.
[18] C.E. Secu, M. Sima, Opt. Mater. 31 (2009) 876–880.
[19] K.R. Nagabhushana, B.N. Lakshminarasappa, F. Singh, Radiat. Measur. 43 (2008) S651–S655.
[20] K.M. Sancier, Surf. Sci. 21 (1970) 1–11.
[21] V.A. Niketenko, J. Appl. Spectrosc. 56 (1994) 783–798.
[22] N.Y. Garces, N.C. Giles, L.E. Halliburton, G. Cantwell, D.B. Eason, D.C. Reynolds, D.D. Look, Appl. Phys. Lett. 80 (2002) 1334–1336.
[23] A. Janotti, C.G. Van de Walle, Phys. Rev. B 76 (2007) 165202.
[24] J.R. Smith, W.H. Vehse, Phys. Lett. 31A (1970) 147–148.
[25] J.M. Meese, D. Galland, Solid State Commun. 11 (1972) 1547–1550.
[26] V. Soriano, D. Galland, Phys. Status Solidi (B) 77 (1976) 739–743.
[27] A.L. Taylor, G. Filipovich, G.K. Lindeberg, Solid State Commun. 8 (1970) 1359–1361.
[28] D. Galland, A. Herve, Phys. Lett. A 33 (1970) 1–2.
[29] D. Galland, A. Herve, Solid State Commun. 14 (1974) 953–956.